Available online at www.sciencedirect.com

SCIENCE DIRECT®

Surface Science 566–568 (2004) 1057–1062

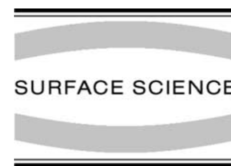

www.elsevier.com/locate/susc

Vertical coupling effects and transition energies in multilayer InAs/GaAs quantum dots

Yiming Li [a,b,*]

[a] *Department of Computational Nanoelectronics, National Nano Device Laboratories, Hsinchu 300, Taiwan*
[b] *Microelectronics and Information Systems Research Center, National Chiao Tung University, Hsinchu 300, Taiwan*

Available online 19 June 2004

Abstract

We investigate the transition energy of vertically stacked semiconductor quantum dots with a complete three-dimensional (3D) model in an external magnetic field. In this study, the model formulation includes: (1) the position-dependent effective mass Hamiltonian in non-parabolic approximation for electrons, (2) the position-dependent effective mass Hamiltonian in parabolic approximation for holes, (3) the finite hard-wall confinement potential, and (4) the Ben Daniel–Duke boundary conditions. To solve the nonlinear problem, a nonlinear iterative method is implemented in our 3D nanostructure simulator. For multilayer small InAs/GaAs quantum dots, we find that the electron–hole transition energy is dominated by the number of stacked layers. The inter-distance d plays a crucial role in the tunable states of the quantum dots. Under zero magnetic field for a 10-layer QDs structure with $d = 1.0$ nm, there is about 30% variation in the electron ground state energy. Dependence of the magnetic field on the electron–hole transition energy is weakened when the number of stacked layers is increased. Our investigation is constructive in studying the magneto-optical phenomena and quantum optical structures.
© 2004 Elsevier B.V. All rights reserved.

Keywords: Computer simulations; Magnetic phenomena (cyclotron resonance, phase transitions, etc.); Quantum effects; Tunneling; Indium arsenide; Gallium arsenide; Heterojunctions

1. Introduction

Nanoscale semiconductor quantum dots (QDs) have been of great interest and successive investigation from both the experimental and theoretical point of views in recent years [1–3]. These structures have diverse applications to electronic and optoelectronic devices, such as semiconductor laser, light emitting diodes, single electron transistors, and single photon emitters. We can currently use the advanced nanofabrication technology to consider another degree of freedom along the growth direction for vertically coupled multilayer QDs. One of evident features in this system is the effects of dot-to-dot interactions on the electronic structure, the electronic entanglement, and charge transfer [4–6]. By considering a 2D lateral geometry and 2D confinement potential models, most of previous works have focused on vertically coupled 2-layer QDs [4–8]. However, it is known that these nanostructures have a 3D confinement potential for the carriers and consequently have a discrete

* Present address: P.O. Box 25-178, Hsinchu 300, Taiwan. Tel.: +886-930-330766; fax: +886-3-5726639.
E-mail address: ymli@mail.nctu.edu.tw (Y. Li).

0039-6028/$ - see front matter © 2004 Elsevier B.V. All rights reserved.
doi:10.1016/j.susc.2004.06.052

energy spectrum with ideally delta-like densities of states [9–11] and ultranarrow gain spectrum. Meanwhile, the geometry configurations significantly impact their electronic structure and luminescence properties. Hence, nanoscale details of the QDs topology for energy spectra as well as the evolution of the coupling effect are critical for the development of novel photonic and electronic applications. To thoroughly clarify the electronic structure and tunneling ability, it is necessary for us to investigate the vertically coupled multilayer QDs with a full 3D approach.

We study in this paper the electronic structure of vertically coupled multilayer QDs using a unified 3D model under applied magnetic fields. Our model considers: (1) the position-dependent effective mass Hamiltonian in non-parabolic approximation for electrons, (2) the position-dependent effective mass Hamiltonian in parabolic approximation for holes, (3) the finite hard-wall confinement potential, and (4) the Ben Daniel–Duke boundary conditions [12–17]. The problem is solved numerically with a generalized nonlinear iterative method [15–17]. This iterative method enables us to compute the vertically coupled multilayer QDs electronic structure efficiently [15]. The constructed system in our investigation possesses 10-layer InAs dots embedded into the GaAs matrix. Each ellipsoidal-shaped QDs layer is equally separated by certain inter-distance d. The effects of the number of stacked layers N and d on the electronic structure have explored. For small dots separated by a fixed d, the transition energy is essentially dominated by N. When N increases, the electron transition energy decreases monotonically and tends eventually to a saturated value. For the 10-layer QDs structure with $d = 1$ nm, the variation of ground state energy is significant and it is less dependent on N for the first excited state. We find d plays a crucial role in the tunable states of the QDs. The dependence of magnetic fields ($\boldsymbol{B}$) on the electron transition energy is weakened when N is increased. The results presented in this work show the importance of the 3D modeling and simulation in exploring the nanoscale vertically coupled multilayer semiconductor QDs. It is constructive in the magneto-optical studies and the development of quantum optical devices.

The outline of this paper is as follows. Section 2 states the 3D model for the vertically coupled multilayer QDs structure and the simulation methodology. Section 3 is the results and discussion. Section 4 draws the conclusions.

2. 3D quantum dot model and simulation method

We consider the vertically stacked QDs with the hard-wall confinement potential [12–17]. In a magnetic field the effective mass Hamiltonian for electrons (k = e) and for holes (k = h) is given in the form

$$\widehat{H}_{\mathrm{k}} = \Pi_{r}\frac{1}{2m_{\mathrm{k}}(E,\boldsymbol{r})}\Pi_{r} + V_{\mathrm{k}}(\boldsymbol{r}) + \tfrac{1}{2}g_{\mathrm{k}}(E,\boldsymbol{r})\mu_{\mathrm{B}}\boldsymbol{B}\sigma, \quad (1)$$

where $\Pi_{r} = -\mathrm{i}\hbar\nabla_{r} + e\boldsymbol{A}(\boldsymbol{r})$ stands for the electron momentum vector, ∇_{r} is the spatial gradient, $\boldsymbol{A}(\boldsymbol{r})$ is the vector potential ($\boldsymbol{B} = \mathrm{curl}\ \boldsymbol{A}$), and σ is the vector of the Pauli matrices. For electrons, $m_{\mathrm{e}}(E,\boldsymbol{r})$ and $g_{\mathrm{e}}(E,\boldsymbol{r})$ are the energy- and position-dependent effective mass and the Landé factor, respectively

$$\frac{1}{m_{\mathrm{e}}(E,\boldsymbol{r})} = \frac{2P^{2}}{3\hbar^{2}}\left(\frac{2}{E+E_{\mathrm{g}}(\boldsymbol{r})-V_{\mathrm{e}}(\boldsymbol{r})} + \frac{1}{E+E_{\mathrm{g}}(\boldsymbol{r})-V_{\mathrm{e}}(\boldsymbol{r})+\Delta(\boldsymbol{r})}\right), \quad (2)$$

$$g_{\mathrm{e}}(E,\boldsymbol{r}) = 2\left\{1-\frac{m_{0}}{m_{\mathrm{e}}(E,\boldsymbol{r})}\frac{\Delta(\boldsymbol{r})}{3[E+E_{\mathrm{g}}(\boldsymbol{r})]+2\Delta(\boldsymbol{r})}\right\}, \quad (3)$$

where $V_{\mathrm{e}}(\boldsymbol{r})$ is the confinement potential, $E_{\mathrm{g}}(\boldsymbol{r})$ and $\Delta(\boldsymbol{r})$ stand for position-dependent energy band gap and spin–orbit splitting in the valence band, P is the momentum matrix element, m_{0} and e are the free electron mass and charge. For holes, $m_{\mathrm{h}}(\boldsymbol{r})$ and $g_{\mathrm{h}}(\boldsymbol{r})$ are assumed to be only position dependent. For both the electron and hole, the hard-wall confinement potential in the inner region of each QD (**1**) and environmental crystal matrix (**2**) can be presented as: $V_{\mathrm{k}}(\boldsymbol{r}) = 0$ for all $\boldsymbol{r} \in \mathbf{1}$ and $V_{\mathrm{k}}(\boldsymbol{r}) = V_{\mathrm{k0}}$ for all $\boldsymbol{r} \in \mathbf{2}$, respectively. The Ben Daniel–Duke boundary conditions for the electron and hole wave functions $\Psi(\boldsymbol{r})$ are given by

$\Psi_{k1}(\mathbf{r}_s) = \Psi_{k2}(\mathbf{r}_s)$ and $(\frac{\hbar^2}{2m_k(E,\mathbf{r}_s)}\nabla_{\mathbf{r}})|_{\mathbf{n}}\Psi_k(\mathbf{r}_s) = \text{const.}$, where $\mathbf{r}_s$ denotes the position of the system interface.

Because of the cylindrical symmetry of the system, the wave function for electrons and holes can be represented as $\Psi_k(\mathbf{r}) = \Phi_k(R,z)\exp(il\phi)$ where $l = 0, \pm 1, \pm 2, \ldots$, is the orbital quantum number. It leads to a problem in the (R,z) coordinate, and the Schrödinger equation for electrons (k = e) and holes (k = h) is

$$-\frac{\hbar^2}{2m_{kj}(E)}\left(\frac{\partial^2}{\partial z^2}+\frac{\partial^2}{\partial R^2}+\frac{1}{R}\frac{\partial}{\partial R}-\frac{l^2}{R^2}\right)\Phi_{kj}(R,z) + \left[\frac{m_{kj}(E)\Omega_{kj}^2(E)R^2}{8}+s\frac{\mu_B}{2}g_{kj}(E)\mathbf{B}+\frac{\hbar\Omega_{kj}(E)}{2}l + V_{k0}\delta_{j\mathbf{2}}\right]\Phi_{kj}(R,z) = E\Phi_{kj}(R,z), \quad (4)$$

where $j = \mathbf{1},\mathbf{2}$, $\Omega_{kj}(E) = e\mathbf{B}/m_{kj}(E)$, and $s = \pm 1$ refers to the orientation of the electron spin along z-axis. The Ben Daniel–Duke boundary conditions are $\Phi_{k\mathbf{1}}(R,z) = \Phi_{k\mathbf{2}}(R,z)$ and

$$\frac{1}{m_{k\mathbf{1}}(E)}\left(\frac{\partial\Phi_{k\mathbf{1}}(R,z)}{\partial R}+\frac{df(R)}{dR}\frac{\partial\Phi_{k\mathbf{1}}(R,z)}{\partial z}\right)_{z=f(R)} = \frac{1}{m_{k\mathbf{2}}(E)}\left(\frac{\partial\Phi_{k\mathbf{2}}(R,z)}{\partial R}+\frac{df(R)}{dR}\frac{\partial\Phi_{k\mathbf{2}}(R,z)}{\partial z}\right)_{z=f(R)} \quad (5)$$

where $z = f(R)$ presents the generating contour of the vertically coupled multilayer QDs on the $\{R,z\}$ plane.

We focus here on principal consequences of a 3D approach in modeling of electron states for vertically stacked QDs. We note that any advanced consideration of geometrical effects will produce further corrections to the electron and hole energy spectra. For example, the different dielectric constants (14.5/12.9) in InAs/GaAs heterostructures may leads to a small renormalization of the electron energy (self-energy) [12,13,18,19]. However, it should not affect the main tendencies and behaviors of the state in the structure.

To compute the electron–hole energy states in a vertically stacked ellipsoidal-shaped QDs structure, shown in Fig. 1, we apply the nonlinear iterative method to calculate the self-consistent solution of the multilayer QDs structure. This computer simulation method has been developed for QDs and quantum ring simulation in our recent works [15–17]. Our calculation experiences show this method converges monotonically; it takes only 12–15 feedback iterative loops to meet a given convergence criterion (the maximum norm error $<10^{-12}$ eV) for all energies.

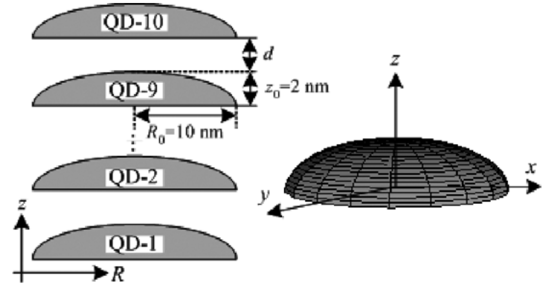

Fig. 1. Cross-sectional plot of the structure consisting of $N = 10$ embedded layers of InAs QDs, separated by a certain inter-distance in GaAs matrix. All InAs QDs are with the 3D ellipsoidal shapes as shown in the right figure.

3. Results and discussion

As shown in Fig. 1, we simulate a 10-layer vertically stacked QDs structure. All InAs dots are with the same ellipsoidal shapes and embedded into the GaAs matrix. Each layer of the ellipsoidal-shaped QD is separated by d equally. The base radius $R_0 = 10$ nm and $z_0 = 2$ nm are adopted for all QDs [20–25]. The material parameters used in our investigation for InAs inside each dot are $E_{1g} = 0.42$ eV, $\Delta_1 = 0.38$ eV, and $m_1(0) = 0.024m_0$. The parameters for GaAs outside of the dots are $E_{2g} = 1.52$ eV, $\Delta_2 = 0.34$ eV, $m_2(V_0) = 0.067m_0$, and $V_0 = 0.53$ eV [26]. Fig. 2 shows the calculated transition energy versus N for the structure with $d = 1$ nm and $\mathbf{B} = 0$ T. For $d = 1$ nm the variation of ground state energy can up to 30%. The transition of the first excited state energy ($|l| = 1$) is less dependent on N ($\approx 14\%$). To clarify the dependence of N on the electron transition energy, we define the occupancy-ratio of electron wave functions $W = \int_{r\in\text{material_1}}\Phi^2(R,z)\,d\mathbf{r}^3/\int_{r\in\text{material_2}}\Phi^2 \times (R,z)\,d\mathbf{r}^3$ for evaluating the probability in finding

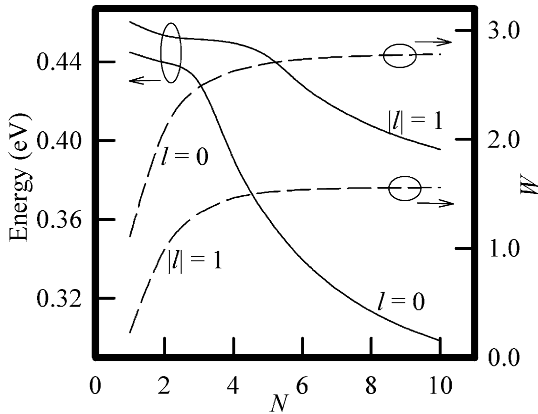

Fig. 2. Electron ground state energy versus N for the structure with $d = 1$ nm and $\boldsymbol{B} = 0$ T. The dash lines indicate the corresponding dependence of the ratio W on N.

the electron inside and outside the QDs. The dash lines indicate the corresponding dependence of the ratio W on N, which becomes independent on N when $N > 6$. As shown in Fig. 3, plots of the calculated wave functions significantly confirm the coupling and spreading effects for the vertically coupled QDs with $N = 1, 2, 5$, and 10. Due to the coupling effect, it is found that the increase of N results in stronger confinement and the energy converges to a stable value shown in Fig. 2. Under $\boldsymbol{B} = 0$ T, Table 1 reports the variation of the electron transition energies $((E_{eN=1} - E_{eN=10})/E_{eN=1})$ for the states of $l = 0$ and $|l| = 1$ in the stacked structure with $d = 0.5, 1, 2, 5$, and 10 nm. In our investigation, it is also found that d plays a crucial role in the tunable states of the dots. For the system with $N = 10$ under $\boldsymbol{B} = 0$ T, we have also estimated that there is more than 25% ground state energy variation when d varies from 0.5 to 10 nm. For the first excited state the energy variation is up to 12%. We have similar observations for different number of layers.

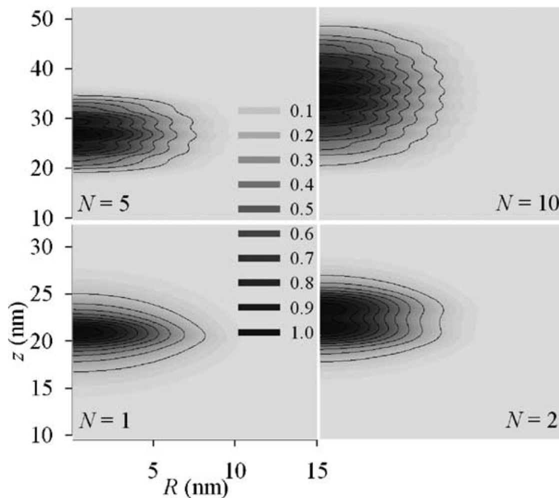

Fig. 3. Contour plots of the electron wave functions for the vertically stacked QDs with $N = 1, 2, 5$, and 10.

Furthermore, for the structure with $d = 1$ nm the electron transition energy among the states is calculated systematically as a function of magnetic fields with arbitrary strength. As shown in Fig. 4, we observed that the dependence of $\boldsymbol{B}$ on the electron transition energy for the case of $l = 0$ is weakened when N increases. The magnetic fields play significant effects on the vertically coupled 2-layer QDs than that on other stacked configurations. For the system consists of only 2-layer QDs, it demonstrates 30 meV energy transition when $\boldsymbol{B}$ varies from 0 to 20 T. For the 10-layer QDs structure the transition is about 5 meV. Fig. 5 shows the ratio W versus N and $\boldsymbol{B}$ for the structure with $d = 1$ nm. For those structures with the small N the electron wave function spreads out of the QDs ($W \approx 1$) and the property of the transition energy is dominated by the band parameters of GaAs matrix. With the same calculation method we have computed the hole energy states, where

Table 1
Variation of the electron transition energies for the cases of $l = 0$ and $|l| = 1$ in a multilayer QDs structure with different inter-distance under $\boldsymbol{B} = 0$ T

Inter-distance d (nm)	0.5	1	2	5	10
Variation of the ground state energy ($l = 0$)	36%	30%	26%	18%	13%
Variation of the first excited state energy ($\|l\| = 1$)	17%	14%	10%	7%	5%

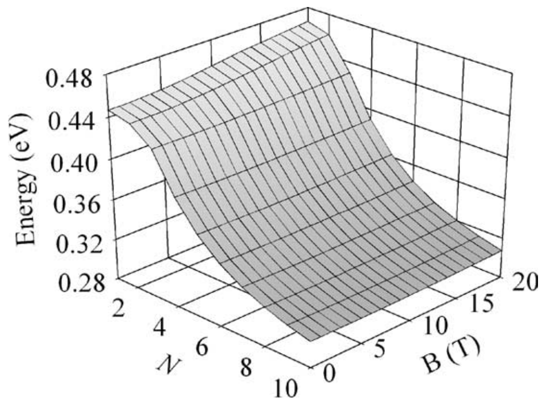

Fig. 4. Electron ground state energy versus N and $\boldsymbol{B}$ for the structure with $d = 1$ nm.

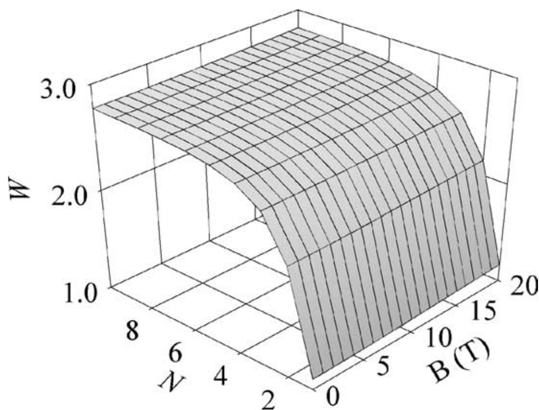

Fig. 5. The structure ratio W versus N and $\boldsymbol{B}$, where $d = 1$ nm.

the hole effective mass was taken as $m_{1h} = 0.4m_0$ and $m_{2h} = 0.5m_0$, respectively; the hole band offset is taken as $V_{h0} = 0.33$ eV [12,13]. The system energy band gap $\Delta E(\boldsymbol{B})$ is equal to $\Delta E_{ge}(\boldsymbol{B}) + \Delta E_{gh}(\boldsymbol{B}) + \Delta E_{gR}(\boldsymbol{B})$, where E_{ge} and E_{gh} are the electron–hole ground state energies, and E_{gR} is the energy gap in the QDs system. The calculated result of the energy gap between the lowest electron and hole states for the stacked 10-layer InAs/GaAs QDs system with the fixed $d = 1$ nm is shown in Fig. 6. For a fixed $\boldsymbol{B}$ we find the energy gap decreases when N increases. The decrease of energy gap flats off when $N > 6$ due to the stable localization effect (weak coupling effect). For $N = 1$ the coupled system becomes a single InAs/GaAs

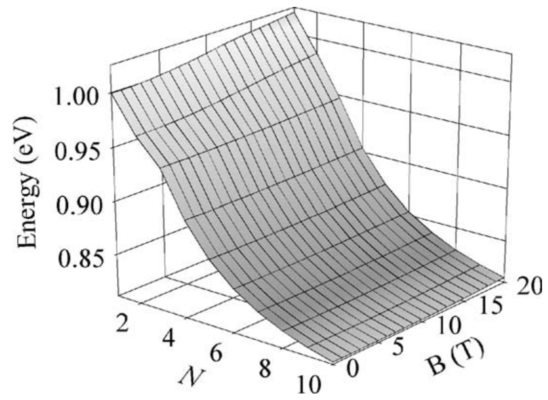

Fig. 6. The energy gap versus N and $\boldsymbol{B}$ for the stacked InAs/GaAs QDs with $d = 1$ nm.

QD and the energy gap variation is mainly from diamagnetic shift [16]. For the system with each $N > 2$ the shift of energy gap is weakened. It is a result of the strong confinement effect for electrons and holes with our correct 3D description. This phenomenon is useful in magnetic-photoluminescence spectra of the nanoscale vertically stacked QDs. However, more detail estimations will be necessary by including the electron–hole Coulomb interaction for those structures with small N and d.

4. Conclusions

In this paper the coupling effects and transition energies have been investigated for the vertically stacked InAs/GaAs QDs under magnetic fields. For small QDs, our 3D model and simulation has shown that the transition energy was directly dominated by the number of stacked layers. The inter-distance between layers also plays a crucial role in the tunable states of the dots. The dependence of magnetic fields on the electron transition energy was depressed when the number of vertically coupled layers is increased. To verify the calculated transition energies of the stacked QDs quantitatively, transition energies can be measured experimentally from the photoluminescence spectra [27–32]. It is believed that this study is useful for the study of quantum optical structures and

design of advanced semiconductor photonic and electronic devices.

Acknowledgements

This work was supported in part by the National Science Council (NSC) of Taiwan under contract nos. NSC-92-2112-M-429-001 and NSC-93-2572-E-009-002-PAE and the Ministry of Economic Affairs, Taiwan under contract no. PSOC 92-EC-17-A-07-S1-0011.

References

[1] H. Akinaga, H. Ohno, IEEE Trans. Nanotech. 1 (2002) 19.
[2] M. Bayer, P. Hawrylak, K. Hinzer, et al., Science 291 (2001) 451.
[3] A.D. Yoffe, Adv. Phys. 50 (2001) 1.
[4] X. Hu, S. Das Sarma, Phys. Rev. A 61 (2000) 062301.
[5] P. Yu, W. Langbein, K. Leosson, Phys. Rev. B 60 (1999) 16680.
[6] Y. Tokura, D.G. Austing, S. Tarucha, J. Phys.: Condens. Matter 11 (1999) 6023.
[7] R. Heitz, A. Kalburge, Q. Xie, et al., Phys. Rev. B 57 (1998) 9050.
[8] B. Partoens, V.A. Schweigert, F.M. Peeters, Phys. Rev. Lett. 79 (1997) 3990.
[9] K. Král, Z. Khás, Phys. Rev. B 57 (1997) R2061.
[10] K. Král, Z. Khás, Phys. Stat. Sol. (b) 204 (1997) R3.
[11] K. Král, Z. Khás, Phys. Stat. Sol. (b) 208 (1998) R5.
[12] G. Bastard, Wave Mechanics Applied to Semiconductor Heterostructures, Halsted Press, Les Ulis, 1988.
[13] S.L. Chuang, Physics of Optoelectronic Devices, Wiley Sons, New York, 1995.
[14] E.A. de Andrada e Silva, G.C. La Rocca, F. Bassani, Phys. Rev. B 55 (1997) 16293.
[15] Y. Li, O. Voskoboynikov, C.P. Lee, et al., Comput. Phys. Commun. 147 (2002) 209.
[16] Y. Li, O. Voskoboynikov, C.P. Lee, et al., Jpn. J. Appl. Phys. 1 41 (2002) 2698.
[17] Y. Li, Int. J. Mod. Phys. C: Comput. Phys. 14 (2003) 501.
[18] P. Vagner, D. Munzar, M. Mosko, Acta Phys. Pol. A 92 (1997) 1038.
[19] M. Mosko, D. Munzar, P. Vagner, Phys. Rev. B 55 (1997) 15416.
[20] E. Steimetz, T. Wehnert, H. Kirmse, et al., J. Cryst. Growth 221 (2000) 592.
[21] H. Eisele, O. Flebbe, T. Kalka, et al., Appl. Phys. Lett. 75 (1999) 106.
[22] B. Lita, R.S. Glodman, Appl. Phys. Lett. 74 (1999) 2824.
[23] Z.R. Wasilewski, S. Fafard, J.P. McCaffrey, J. Cryst. Growth 201/202 (1999) 1131.
[24] J. Martínez-Pastor, B. Alén, C. Rudamas, et al., Physica E 17 (2003) 46.
[25] M. Bayer, G. Ortner, A. Larionov, et al., Physica E 12 (2002) 900.
[26] C. Pryor, Phys. Rev. B 60 (1999) 2869.
[27] M.S. Miller, J.-O. Malm, M.-E. Pistol, et al., J. Appl. Phys. 80 (1996) 3360.
[28] K. Kamath, N. Chervela, K.K. Linder, et al., Appl. Phys. Lett. 71 (1997) 927.
[29] G. Sek, K. Ryczko, J. Misiewicz, et al., Solid State Commun. 117 (2001) 401.
[30] J. Humlicek, D. Munzar, K. Navratil, et al., Physica E 13 (2002) 229.
[31] S. Nomura, Y. Aoyagi, Surf. Sci. 529 (2003) 171.
[32] A. Somintac, E. Estacio, A. Salvador, J. Cryst. Growth 251 (2003) 196.